1st IMEKO TC-4 International Workshop on
Metrology for Geotechnics
Benevento, Italy, March 17-18, 2016

Effectiveness of inhibiting liquefaction triggering by shallow ground improvement methods: field shaking trials with T-Rex at one area in Christchurch, New Zealand

K. H. Stokoe II[1], J. N. Roberts[1], S. Hwang[1], B. R. Cox[1], and F. Y. Menq[1], S. van Ballegooy[2]

[1] *Department of Civil, Environmental, and Architectural Engineering, University of Texas at Austin, k.stokoe@mail.utexas.edu (USA)*
[2] *Tonkin & Taylor Ltd, Auckland (New Zealand)*

***Abstract* – Christchurch and the Canterbury region in New Zealand were devastated in 2010-2011 by a series of powerful earthquakes. The Christchurch area experienced widespread liquefaction that caused extensive damage. One critical problem facing the rebuilding effort is that the land remains at risk of liquefying in future earthquakes. Therefore, effective engineering solutions had to be developed to increase the resilience of homes and low-rise structures. To this end, a comprehensive series of full-scale field trials of multiple shallow ground improvement methods was performed. The field trials presented in this paper were conducted at one area in a severely damaged suburb of Christchurch and involved five test panels of different ground improvements. Each test panel and two additional test panels of unimproved natural soil were instrumented with embedded arrays of sensors and were characterized by crosshole seismic testing before shaking. A large mobile shaker, called T-Rex, was used to perform a staged-loading sequence of increasing sinusoidal horizontal loads at the surface of each test panel. The results of the staged-loading tests were successfully used to identify ground improvement methods that improved the ground performance versus those methods that contributed an insignificant improvement or even degraded the ground performance. The results of the pre-shaking crosshole tests were successfully used for two purposes. First, portions of the soils below the water table that were unsaturated were identified using compression wave velocities. Second, shear wave velocities were used: (1) to identify changes in the natural soil skeleton between improvements, and (2) to evaluate the effective shear stiffness of the combined improvement and surrounding natural soil. Further, the crosshole measurements led to development of a field verification method for use in evaluating changes created by shallow ground improvements.**

I. INTRODUCTION

In 2010-2011, the city of Christchurch, New Zealand was devastated by a series of powerful earthquakes, including six significant events. The most destructive of these events were the 4 September 2010, moment magnitude (MW) 7.1, Darfield Earthquake and the 22 February 2011, MW 6.2, Christchurch Earthquake. The proximity to the city, shallow depth, and fault mechanism of the Christchurch Earthquake generated the largest ground motions in the city, with horizontal peak ground accelerations (PGAs) between 0.37 and 0.52 g recorded in the Central Business District (CBD). As discussed by Cubrinovski et al. (2012), the 2010-2011 earthquakes caused repeated liquefaction throughout the suburbs of Christchurch and the CBD. They noted that the liquefaction was very severe and widespread (covering nearly one third of the city area) and caused extensive damage to the built and natural environments. Interestingly, it was reported by some residents that liquefaction severity increased in subsequent events.

One critical problem facing Christchurch and the Canterbury region is rebuilding on land that remains at risk of liquefying in future earthquakes. Bowden et al. (2012) have noted that "there is a need to develop simple, cost-effective engineering measures which increase the resilience of new houses to limit losses and disruption from future earthquakes." To this end, several field test trials of full-scale, shallow, ground improvement methods were performed in 2011 and 2012 to assess their effectiveness for use in improving residential foundation performance. The full-scale field trials used dynamic loading created by explosive charges (blasting) to induce liquefaction. As summarized in a report by Tonkin and Taylor (2013), the field trials generally "showed that undertaking shallow ground improvements increased site performance and decreased liquefaction vulnerability."

ISBN: 978-92-990075-0-1

With information from the blast-loading field trials, Tonkin and Taylor decided in early 2013 to perform a comprehensive series of full-scale field trials of multiple types of shallow ground improvement methods. The field trials involved evaluating the ground improvements under two different loading conditions: (1) initially with a large mobile shaker, called T-Rex, on the ground surface, and (2) then with explosive charges placed at depth. The purpose of the field trials was to determine if and which improvement methods achieve the objectives of inhibiting liquefaction triggering in the improved ground and are cost-effective measures. This knowledge is needed to develop foundation design solutions in areas outside the "Red Zone," the zone where structures will not be rebuilt, as well as for the repair of damaged land. This effort has been sanctioned by four New Zealand authorities (Earthquake Commission (EQC), Housing New Zealand (HNZ), Canterbury Earthquake Recovery Authority (CERA), and Ministry of Business Innovation and Employment (MBIE)) to be part of formulating the path forward in rebuilding the infrastructure in Christchurch and the Canterbury region.

In this paper, staged-loading field trials using T-Rex at one of three test areas in the suburbs around Christchurch are presented. This work is a small part of a much larger testing program that began in spring 2013 with a preliminary evaluation of seven potential test areas along the Avon River within and around Christchurch. From the seven potential areas, three areas were selected for the field trials based on their geotechnical characteristics, their similarity to future areas that will undergo ground improvements, and how readily and cost-effectively the candidate ground improvements could be installed and tested at each test area. The test area discussed herein is called Site 6 hereafter. The information presented in the paper covers: (1) the four types of ground improvement methods that were investigated at Site 6, (2) the test panels that were created with the ground improvements as well as two natural soil test panels, (3) installation of an embedded sensor array in the central region of each test panel that was used to monitor ground motions and pore-water pressure generation during shaking, (4) characterization of the unimproved and improved ground conditions at the test panels before shaking, (5) example records of pore-water pressure generation and shear strain during shaking, and (6) observations of the effectiveness or ineffectiveness of each ground improvement method.

II. FULL-SCALE GROUND IMPROVEMENT METHODS INSTALLED AT SITE 6 AND ASSOCIATED GROUND CONDITIONS

A. Selected ground improvement methods

Four ground improvement methods were selected by Tonkin and Taylor for the full-scale field trials at Site 6. The improvement methods are shown in Figure 1. They are: (1) Rapid Impact Compaction (RIC), also known as dynamic compaction, Figure 1a, (2) Rammed Aggregate Piers (RAP), which consist of dense gravel columns, Figure 1b, (3) Low Mobility Grouting (LMG) with a cement paste, also referred to as compaction grouting, Figure 1c, and (4) construction of a single row of horizontal beams (SRB) or a double row of horizontal beams (DRB) beneath existing residential structures via soil-cement mixing, Figure 1d. The RIC, RAP, and LMG methods were constructed as they would be used in the reconstruction effort; hence, the term "full-scale" field tests. Each improvement was designed to extend to a depth of about 4 m. All horizontal beams were: (1) 0.5 m in diameter, (2) made of moderate stiffness, fine-aggregate concrete, and (3) positioned with a minimum of 0.5 m of soil cover over either the SRB or DRB. The beams were also constructed as expected in the reconstruction effort, so "full-scale" testing was performed. More information about the ground improvement methods can be found in van Ballegooy et al. (2015b).

B. Generalized site area and test panels

Site 6 was located within 30 m of the Avon River near the Pages Road Bridge in the suburb of Bexley. The plan dimensions of Site 6 were about 50 by 60 m. Seven test panels, each nominally 9 by 9 m, were distributed around the site as shown in Figure 2. The seven test panels were the RIC, RAP, LMG, SRB, DRB, and two unimproved (natural) soil areas. Each test panel was identified by the site number, type of ground improvement or ground condition, and number of the panel. As an example test panel, 6-NS-1 is Site 6, natural soil, and panel 1 of the natural soil. At this site, there were two test panels of natural soil but only one test panel of each ground improvement condition. Ample space existed at Site 6 to allow construction and testing equipment to move around the site without disturbing the test panels.

The soil profile at each test panel was determined after completion of all pre-shaking site characterization by in-situ cone penetration testing (CPT) and small-strain crosshole testing and after completion of the staged-loading shaking tests with T-Rex. (The CPT test results are not presented in this paper but can be found in Van Ballegooy et al. 2015b.) Each soil profile was determined by dewatering the test panel, trenching along the centerline to a depth that ranged between 2.5 and 3.5 m, logging and photographing the trench wall, and recovering disturbed samples for laboratory testing. The soil profile varied somewhat from panel to panel, with the number of layers ranging from 4 to 5. As an example, the 3-m deep soil profile at the 6-NS-1 test panel is:

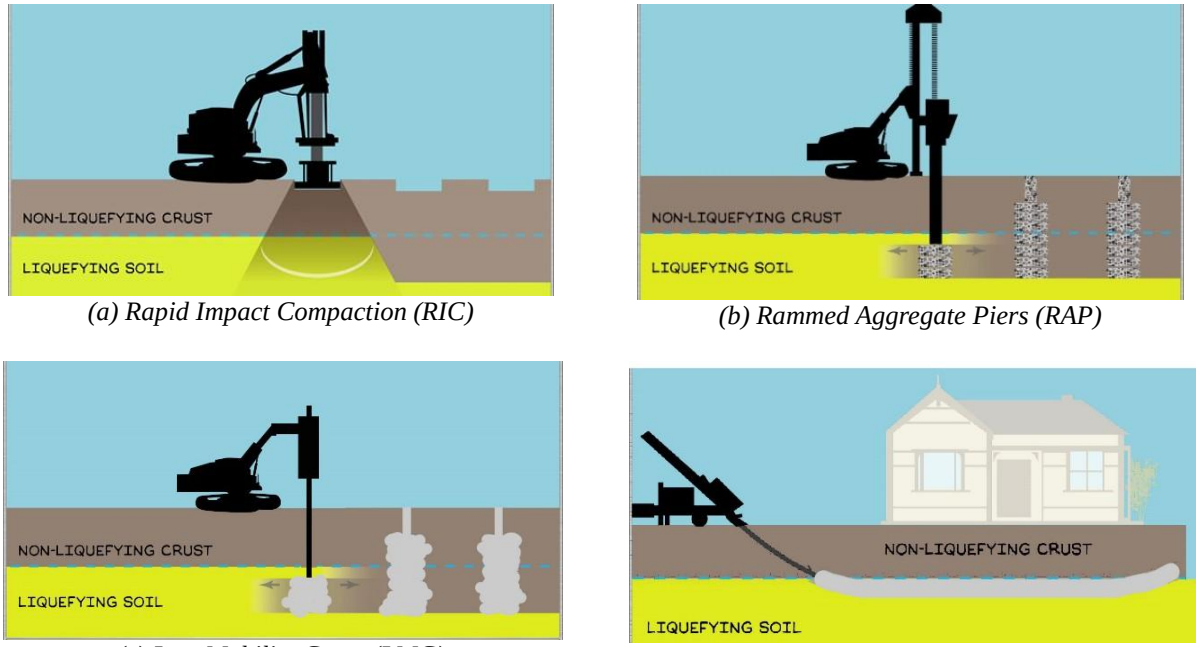

(a) Rapid Impact Compaction (RIC)

(b) Rammed Aggregate Piers (RAP)

(c) Low Mobility Grout (LMG)

(d) Single Row or Double Row of Horizontal Beams (SRB or DRB)

Figure 1: Illustration of the four ground improvement methods evaluated in the field trials at Site 6.

Layer 1 – fine to medium sand with some organics (thickness ≅ 0.70 m),

Layer 2 – silt with trace organics; non-plastic, stiff (thickness ≅ 0.45 m),

Layer 3 – sandy silt; non-plastic, stiff (thickness ≅ 0.35 m), and

Layer 4 – silty fine sand; loose to medium dense; reducing silt content with depth; and extending beyond 5 m as indicated by other site investigations.

The silty fine sand in Layer 4 is the soil that liquefied during multiple earthquakes and produced significant surface ejecta at Site 6. The gradation characteristics of this soil from depths of 2.0 and 3.0 m are: D_{50} ≅ 0.19mm, D_{10} ≅ 0.12mm, and C_u ≅ 1.7, and less than 5% fines (Wang, 2015). The Unified Soil Classification symbol for this silty sand is SP.

III. INSTRUMENTING THE TEST PANELS AND PRE-SHAKING CHARCTERIZATION OF THEM

A. Instrumenting the test panels before shaking with T-Rex

Before performing the T-Rex shaking tests, an array of embedded sensors had to be constructed within each ground improvement and natural soil test panel. The plan dimensions of the loading platen of T-Rex (typically referred as the baseplate) is 2.3 by 2.3 m. All embedded instrumentation was placed within the footprint of the baseplate at each test panel. Nearly all instrumentation was installed by the UTexas crew using the pushing mechanism at the rear of T-Rex (see Figure 3a). The arrangement of the embedded instrumentation in the five test panels without horizontal beams is shown in cross section in Figure 3b and in plan view in Figure 3c. The instrumentation was composed of four, 2D velocity transducers (also called 2D geophones) and five, pore-water pressure transducers (PPTs). As seen in Figure 3c, the instrumentation was located in the central portion of the test panel in soil between the ground improvements. The relative location of the baseplate of T-Rex on the complete RAP test panel is shown in Figure 3d and in a cross-sectional perspective in Figure 4.

Fewer sensors were installed in the SRB and DRB test panels and their locations were somewhat different because of obstructions created by the beams. Vertical and horizontal perspective views of these test panels and instrumentation can be found in Wansbone and van Ballegooy (2015).

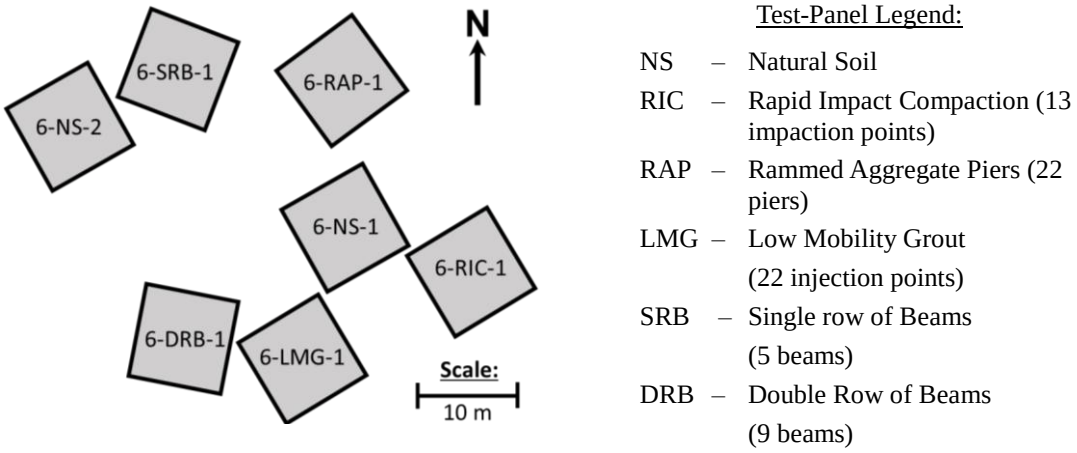

Figure 2: Test area at Site 6 with the relative locations of the seven test panels shown.

B. Motivation for small-strain crosshole seismic testing before shaking

Crosshole seismic testing was used to determine profiles of constrained compression wave velocity, Vp, and shear wave velocity, Vs, to characterize the five test panels (RIC, RAP, LMG, SRB, and DRB) after construction and before shaking with T-Rex. The two natural-soil test panels were protected from the construction activities and were also characterized so that these panels could be used to represent the unimproved natural ground at Site 6. The pre-shaking crosshole testing formed a critical part of the characterization of each test panel for three reasons. First, the Vs profiles of the unimproved (natural) ground were compared with the Vs profiles at each improvement panel to evaluate: (1) the "average" stiffness of the improved zone which, in principle, included the improvement and some soil around the improvement (Zone A in Figures 3c and 5) and (2) any changes in the soil in the "unimproved" zone between the improvements which occurred due to construction of the improvements (Zone B in Figures 3c and 5). (Note, the term "unimproved" in quotes is used to indicate the possibility that this zone has also been changed by construction of the surrounding improvements in the test panel.) Second, overburden-stress corrected Vs values were used to estimate liquefaction triggering susceptibility using Andrus and Stokoe (2000) and Kayen et al. (2013). Third, the Vs values were also helpful in estimating the overall stiffness of each test panel.

The Vp profiles were used for two purposes. First, and most importantly, the Vp values were used to determine at what depths the soil was either fully saturated or nearly saturated (Sr > 99.7 %) so that the dynamic pore pressure measurements would be correctly interpreted; that is, if Sr < 99.7 %, then little to no pore pressure generation would likely occur but it would not be misinterpreted as representing a denser, non-liquefiable soil. The use of Sr of 99.7% to separate behaviour will be studied more in the future and is only used to begin the studies presented herein. The value is based on studies conducted by Valle-Molina (2006) and Valle-Molina and Stokoe (2012). Second, when the degree of saturation is low enough, Poisson's ratio of the soil skeleton will be calculated using the values of Vs and Vp in further work in this study and in future studies.

C. Crosshole seismic testing arrangement and example records

The generalized crosshole testing arrangement, illustrated in Figure 5, involved pushing two dummy CPT cones, one on either end of a linear array. The cones and associated rods were used to transmit vertical impulses to the bottom of the rods where the cone tips acted as sources of both compression (P) and shear (S) waves in these small-strain tests. At the same time, a 3D velocity transducer was pushed in the center of the array using T-Rex. The 3D velocity transducer acted as the receiver for each seismic source. The spacing between the sources at each end and the middle 3-D receiver ranged from about 1.2 to 1.8 m.

Crosshole testing began at a depth of 40 cm and continued in 20-cm increments, usually to a final depth of 5 m. Both seismic source rods and the 3D receiver were pushed to the same depth for each measurement. The reason for the two measurement paths (source #1 (S1) to the receiver (R) and source #2 (S2) to the receiver (R)) is that one path was positioned within the "unimproved" soil zone between improvements while the second path was across the improved zone at the test panels with

(a) Installing 2D velocity transducers (geophones) and pore pressure transducers (PPTs) with the hydraulic ram on the back of T-Rex.

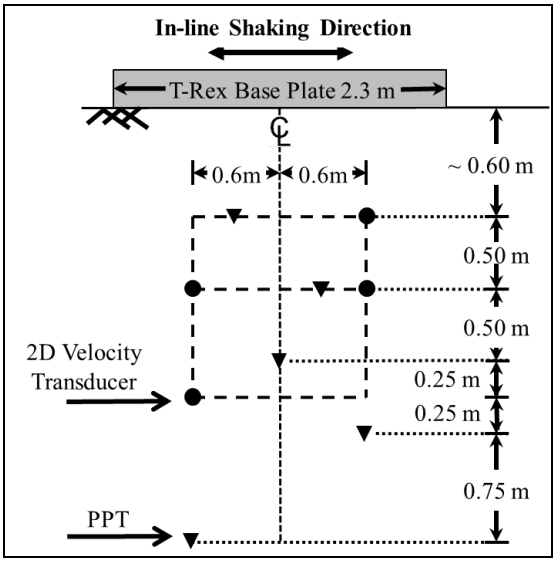

(b) Instrumentation array created in soil subsequently shaken by T-Rex; approximate locations projected on a vertical plane.

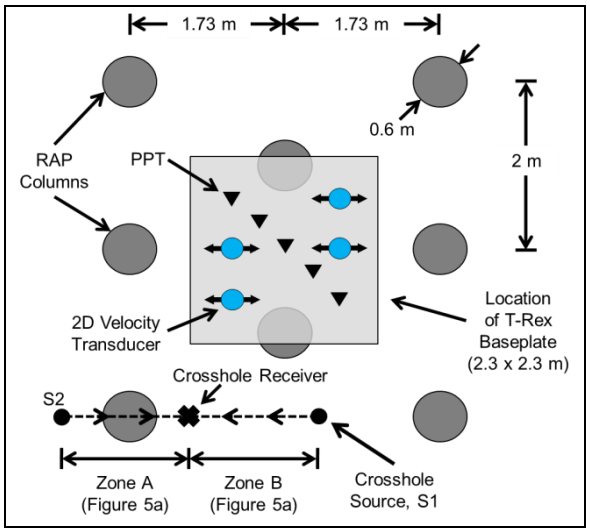

(c) Plan view of central portion of RAP test panel with locations of T-Rex baseplate and pre-shaking crosshole seismic tests.

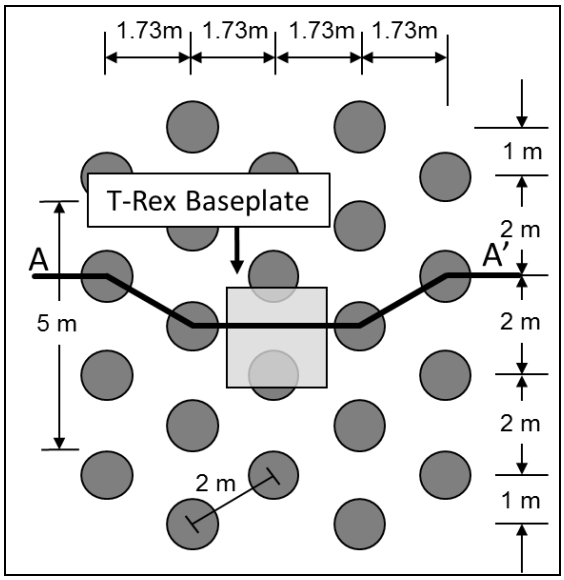

(d) Plan view showing the complete RAP test panel with 22 RAP columns, the location of the T-Rex baseplate, and cross-section A-A' used in Figure 4.

Figure 3: Example showing: (a) installation of embedded sensors at the RAP test panel, (b) relative vertical locations of the sensors beneath the T-Rex baseplate (c) relative horizontal locations of the sensors beneath the T-Rex baseplate and the location of the pre-shaking crosshole tests, and (d) location of T-Rex on the complete RAP test panel during shaking and cross-section A-A' used in Figure 4.

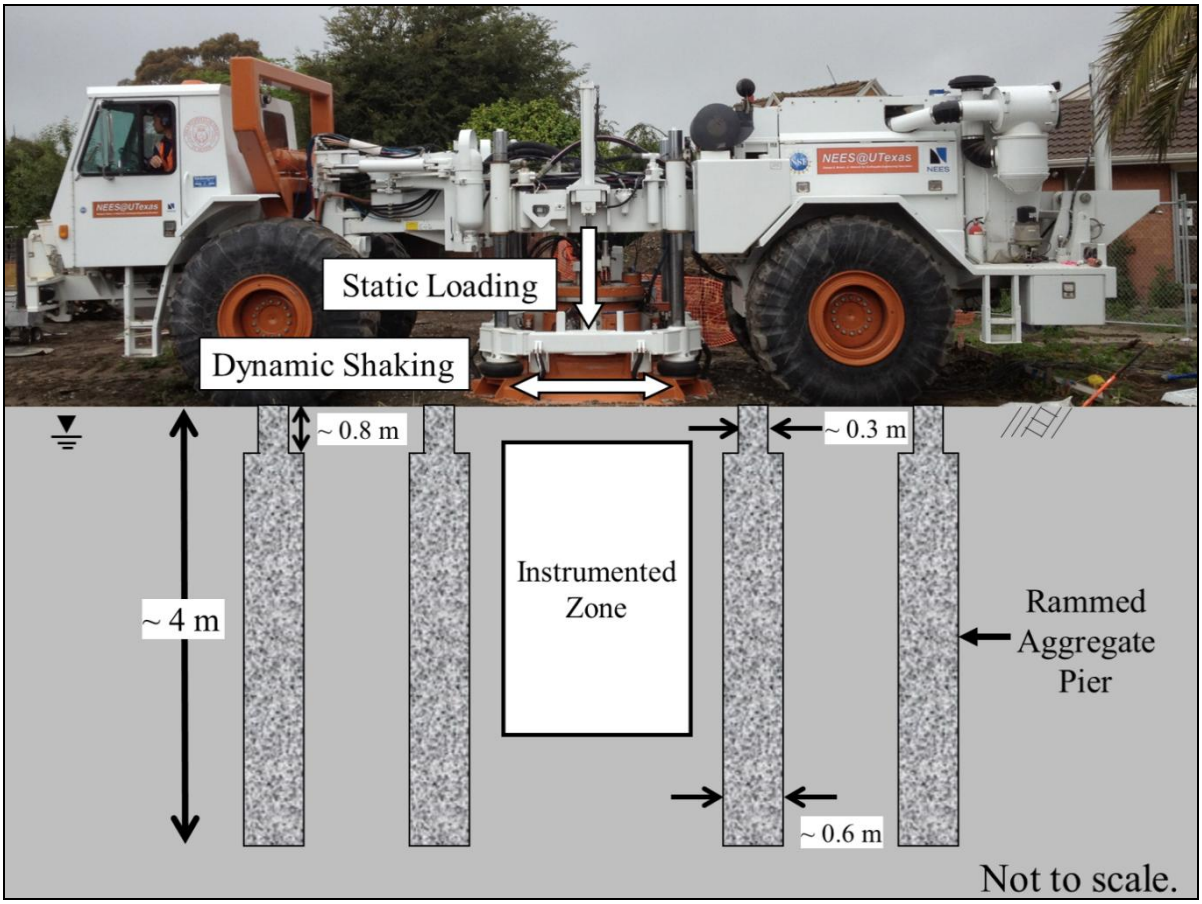

Figure 4: Cross-sectional perspective (Section A-A' in Figure 3d) of T-Rex in place to shake the RAP test panel.

improvements. These two zones are shown in Figures 5a and 5b as Zones A and B for the improved and "unimproved" areas, respectively. (The relative location of the crosshole testing to the embedded sensor array is shown in Figure 3c.) At the two Natural Soil test panels, the same source-receiver arrangement was employed which resulted in each travel path occurring in unimproved, natural soil.

Example trigger, P- and S-wave records at one depth (3.2 m) in natural soil test panel 6-NS-1 are shown in Figure 6. The three waveform records are averaged records from 3 to 5 downward hits of a small hand-held hammer to the top of one of the source rods. The top waveform record is the accelerometer on the source hammer, and time zero on the horizontal time scale is the initial impact of the hammer. The middle and bottom waveforms are the P- and S-wave records, respectively. Each of the records have been corrected for the time required by the compression wave propagating from the top to bottom of the source rod. In this case, a high-frequency signature in the P-wave record is shown, and the initial arrival, denoted by "P", is easily identified. The high-frequency signature is indicative of a saturated condition and is easily achieved when the source CPT rod is lightly struck on the top with the small hammer. The corrected P-wave travel time is identified as Δt_p. The shear wave record also shows a strong initial arrival, identified by "S", from which the S-wave travel time (Δt_s) is readily determined. In the case of these records, the wiring of the vertical geophone results in an upward swing (positive voltage) in the S-wave record at the initial arrival time, and the wiring of the horizontal, radial geophone results in a downward swing (negative voltage) in the P-wave record at the initial arrival time.

Complete sets of P- and S-wave records for the 6-NS-1 test panel are presented in Figures 7 and 8, respectively. Each record set is presented as a waterfall plot, and the wave arrival times are identified by the "dots" on the records.

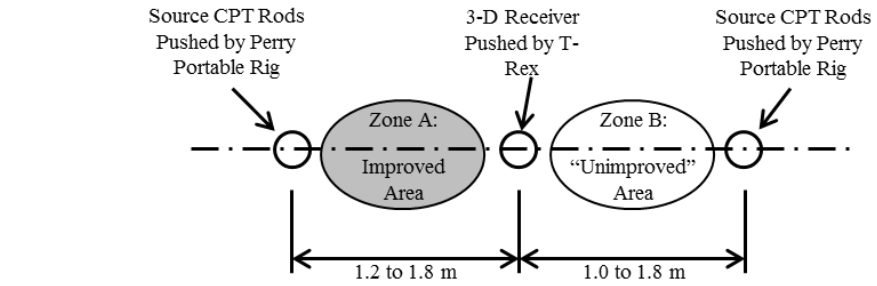

(a) Plan View

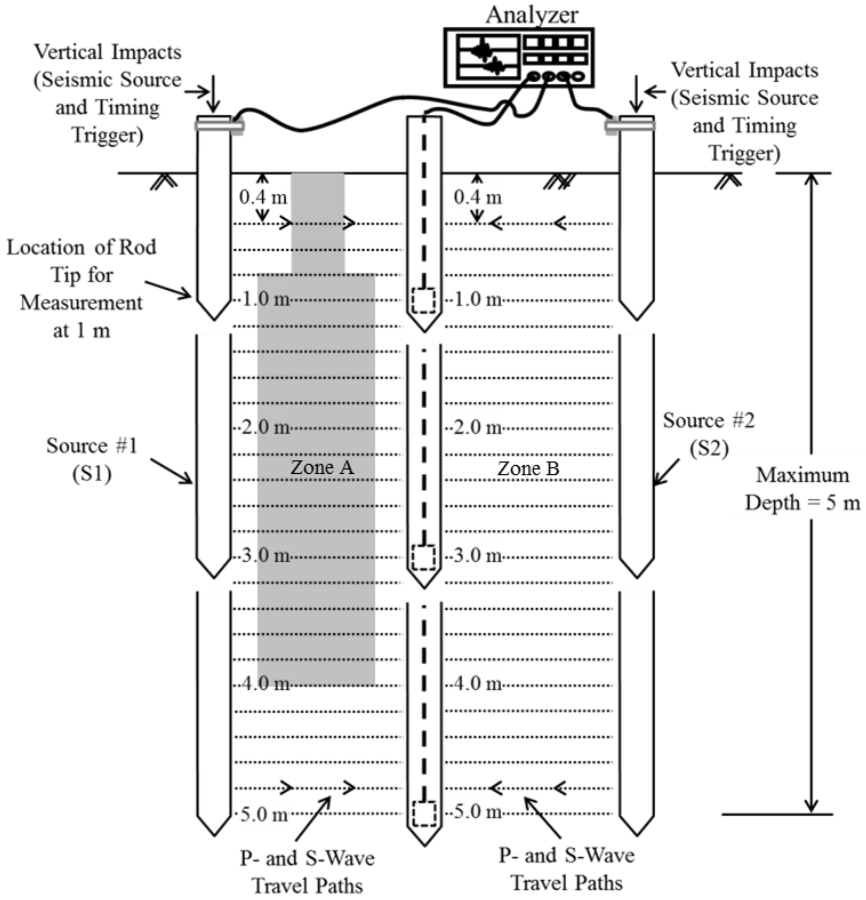

Notes: 1. Zone A is the improved area over some depth range which includes the improvement and some surrounding soil.
2. Zone B is the "unimproved" area between improved areas which may have been changed somewhat by the improvement.

(b) Cross Section

Figure 5: Schematic of generalized arrangement for small-strain crosshole seismic testing at Site 6: (a) using two seismic sources and one, 3D receiver in the middle portion of the test panel, and (b) performing testing in 20-cm depth intervals, beginning at a depth of 40 cm and extending to a depth of 5 m.

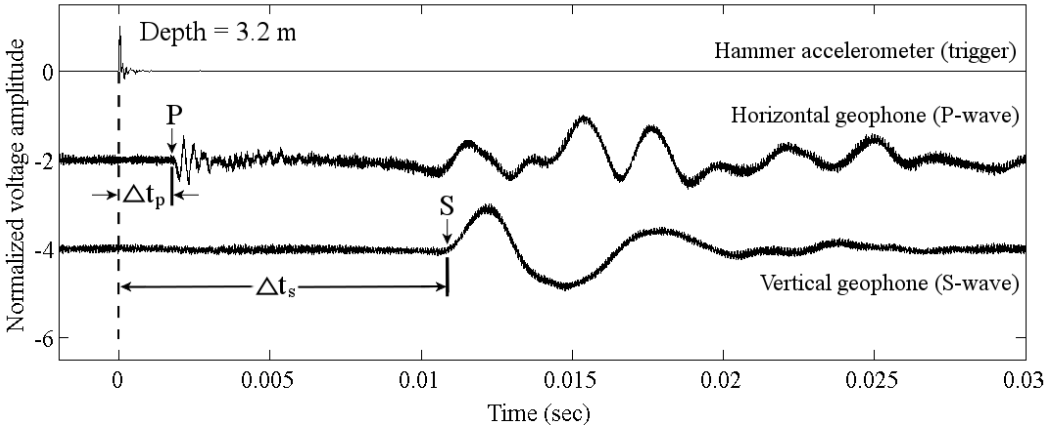

Figure 6: Travel-time records of compression (P) and shear (S) waves at one of the natural soil test panels at Site 6 (6-NS-1 in Figure 2). Example travel-time records with wave arrivals and associated corrected travel times in the soil ae identified on the P and S waveforms. (Note: Relative location of crosshole testing is shown in Figure 3c.)

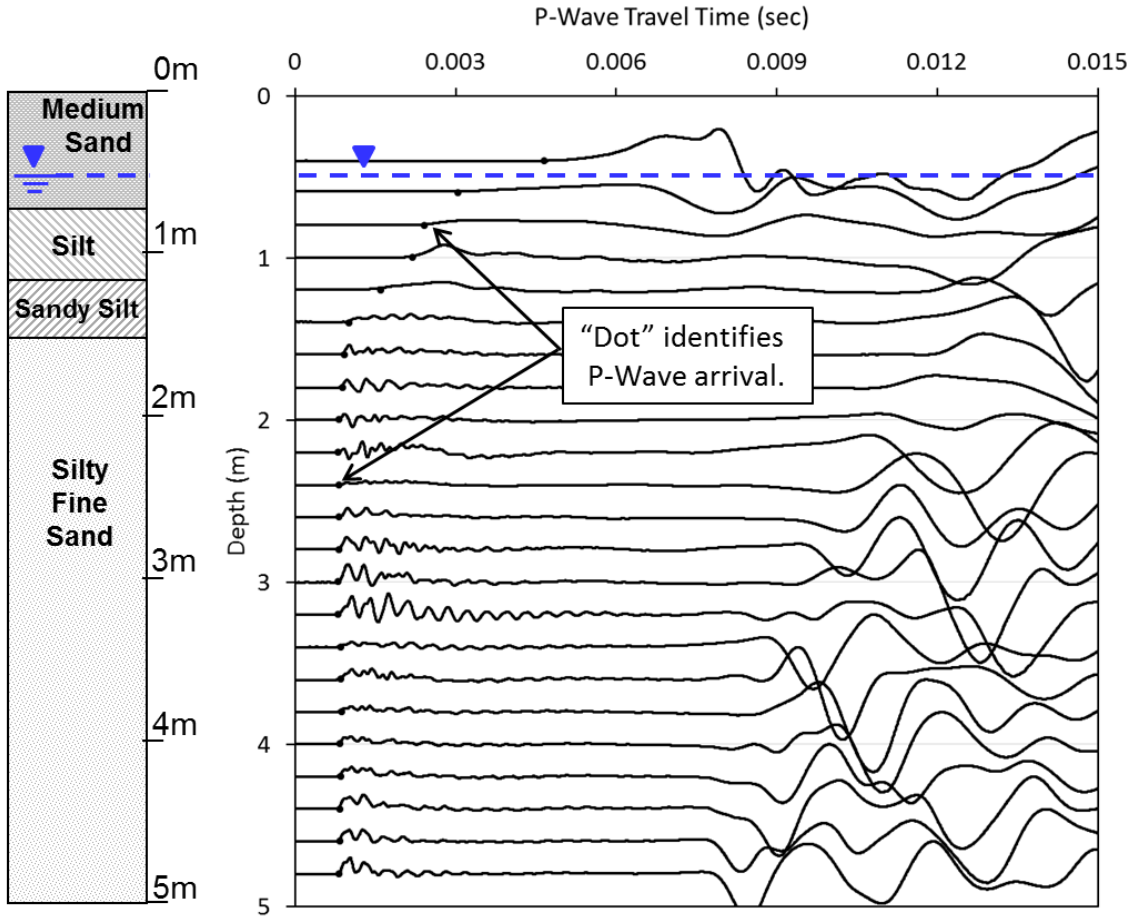

Figure 7: Complete set of P-wave, travel-time records measured at the 6-NS-1 test panel with the P-wave arrival identified on each waveform. (Note: All travel records have been corrected for travel time in the source rod.)

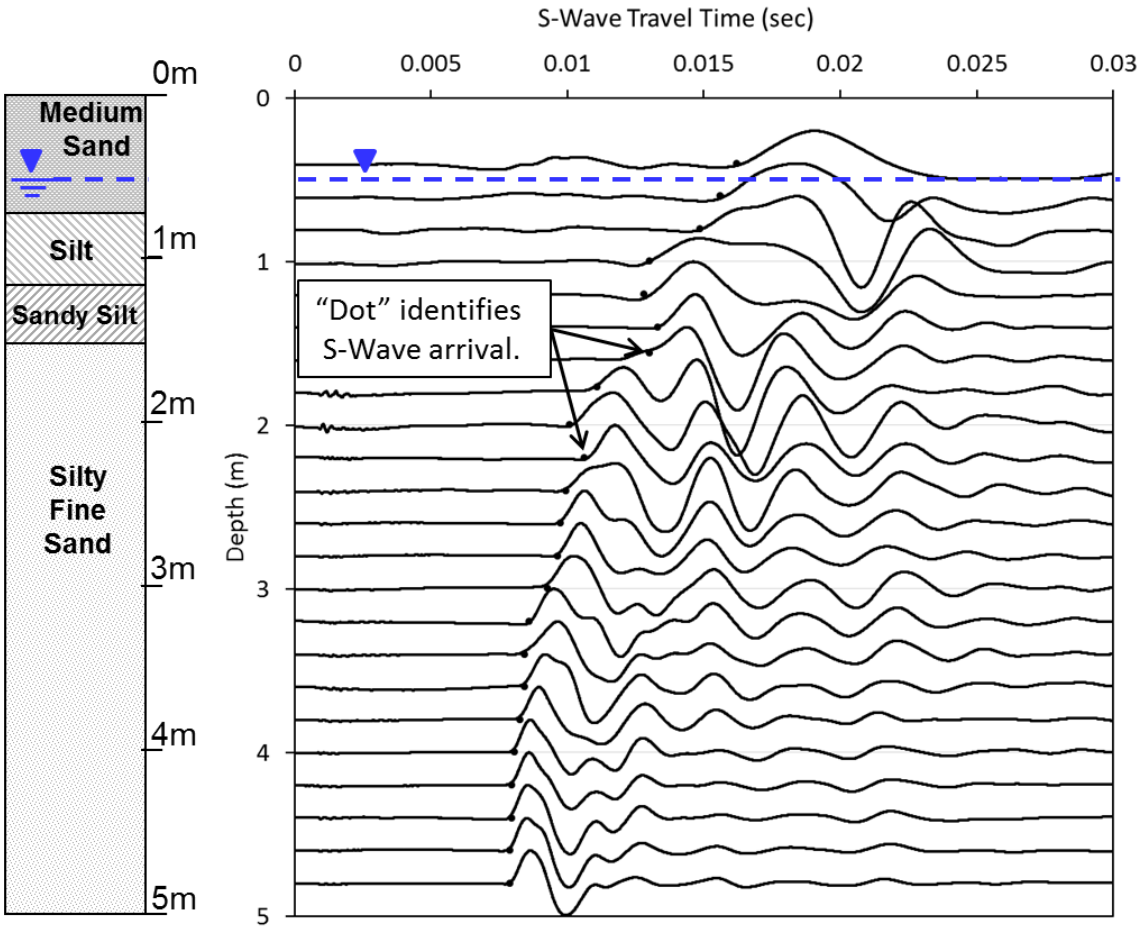

Figure 8: Complete set of S-wave, travel-time records measured at the 6-NS-1 test panel with the S-wave arrival identified on each waveform. (Note: All travel records have been corrected for travel time in the source rod.)

The soil profile has also been added on the left-hand side of each figure. The waterfall plots clearly show how the travel times, hence wave velocities, change with depth. As noted above, the travel times have been corrected for the travel time in the source rod. Also, the initial breaks in the P-wave records in Figure 7 are upward compared with the downward break shown in Figure 6. This difference simply results from different directions of propagation of the P-wave; that is in Figure 6 it is S1 to the horizontal, radial receiver and in Figure 7 it is S2 to the same horizontal, radial receiver. (See plan view in Figure 3c for the relative locations.) These results and discussion also highlight the need to know the orientation and polarity of each geophone in the crosshole 3-D receiver.

D. Crosshole seismic testing reults

D.1 P-wave veocities

The P-wave velocities were measured to identify three different levels of saturation in the soil. These three levels are associated with pore-water pressure generation (or the lack of generation) during shaking. The first level is when the soil is saturated. This condition is represented by Vp in the range of about 1,450 to 1,700 m/s in the silty fine sand (SP) at Site 6. The second condition is when the soil is nearly saturated; that is, the degree of saturation is greater than about 99.7 % (Valle-Molina and Stokoe, 2012). This condition is represented by Vp between about 600 and 1,450 m/s. For these two conditions, loose sandy soils will generate large pore-water pressure leading to liquefaction. The third condition is when the soil is unsaturated and Vp is less than 600 m/s. In this case, the water in the sandy soil at Site 6 has a moderate to small effect on Vp which results in a low likelihood of generating significant pore-water pressure during earthquake shaking for level-ground conditions. At Site 6, the shaking tests described in Section 4 showed that there was no likelihood of liquefaction in the sandy soil when Vp < 600 m/s.

The Vp profiles in the test panels at Site 6 show a significant range in P-wave velocities in the top ~3m as seen in Figure 9a. The one common characteristic is that all profiles show the sandy soil to be unsaturated over some depth below the water table, and the water table averaged about 0.48 m below the ground surface as discussed below. The depth at which 100% saturation occurred ranges from as little as 1.3 m as shown in Figure 9b for the NS, RAP and SRB test panels to as much as 2.8 m for the LMG test panel as shown in Figure 9c. At the RIC and DRB test panels, there was a perched, 100% saturation zone in the depth range of about 1.6 to 2.0 m (Figure 9d). An unsaturated zone that was 0.5 to 1 m thick underlaid this zone but, this "unsaturated" zone likely had $S_r \geq 99.7\%$. Below 2.8 m, the soil at the RIC and DRB test panels was 100% saturated. As a note, identification of 100% saturation was readily done because it was based on a high–frequency signature in the P-wave record, as shown in Figure 6. Such records always resulted in $Vp \geq 1{,}450$ m/s.

The average depth of the water table during seismic testing at each test panel was measured with a piezometer near the center of Site 6. The average water table depth during the 10 days of testing averaged about 0.48 m below the ground surface. The distance below the water table to the point at which 100% saturation was continuous (not perched) ranged from about 0.82 to 2.32 m.

D.2 S-wave veocities

The Vs profiles at the two natural soil panels are shown in Figure 10a. A median profile is also shown and is used for comparison with Vs profiles at the five, improvement test panels. The range in Vs values from the median profile averaged about +/- 8%. This variation is quite reasonable considering the variability in the material found during logging the trenches at the test panels after all testing was completed (van Ballegooy et al., 2015b).

The Vs profiles of the "unimproved" ground between the improvements at the RIC, RAP, SRB and LMG test panels are presented in Figure 10b and are compared with the median profile of the natural soil. No profile is shown for the DRB because measurements could not be performed between the beams in the double row of beams. The profile in Figure 10b shows the following. First, the soil between improvements at the RIC and RAP test panels was stiffened over much of the profile, even extending below 4 m, the bottom of the RAP. Second, the "unimproved" zone between the beams in the SRB test panel has the same Vs profile as the median profile of the Natural Soil test panels. Hence, installation of the SRB did not affect the surrounding soil. Finally, the low Vs values in the zone between the LMG columns show that zone was disturbed, mainly in the depth range of 2 to 3.5 m. This disturbance probably was caused by high injection pressures fracturing the shallow soil that was under low confining stresses. Additional studies are warranted to understand more completely the reasons for the disturbance and possible modifications to improve the application of the LMG method.

In Figure 10c, the Vs profiles around the SRB and DRB test panels are presented. In this case, the measurements are made in a direction perpendicular to the orientation of the beams. The Vs values are generally increased at shallow depths, likely due to some sampling of the beam(s). Below the beams, the DRB test panel even showed a decrease which has not been found at the other two test sites under evaluation. In Figure 10d, the improved zones at the RIC, RAP and LMG test panels are compared with the median Vs profile of the Natural Soil test panels. The RAP improved zone shows significant improvement over the total depth of 5 m and the most improvement of any method below 1.8 m. The LMG improved zone shows good improvement from 0.4 to 3.6 m. The RIC improved zone shows some improvement in the depth range of 1.4 to 4.8 m, an increase of almost 10% in Vs. This moderate increase in Vs at the RIC test panel did significantly change the liquefaction triggering performance as discussed below.

IV. RESULTS OF SHAKING TESTS WITH T-REX

The relative effectiveness of the ground improvement methods to inhibit liquefaction triggering was evaluated by dynamically loading the ground surface at each test panel with T-Rex and monitoring the movements and dynamic pore-water pressures in the loose silty sand with embedded sensors. The sensor array was located in the soil between the ground improvements as shown in Figures 3 and 4. T-Rex was operated by the Geotechnical Engineering Center at The University of Texas at Austin and was used to perform controlled shaking in a staged-loading sequence over a wide range of shaking levels. At each test panel, the dynamic loading from T-Rex was: (1) horizontally oriented, (2) applied at 10 Hz for 100 cycles (10 seconds of shaking), and (3) performed in stages, going from the lowest level (± 13 kN) to the highest level (± 107 or ± 133 kN), normally in five stages. The PPT output is expressed as a pore-water pressure ratio, r_u, that equalled the excess pore-water pressure (u) divided by the initial vertical effective stress which included the vertical loading from T-Rex. The shear strain at each PPT was estimated using the displacement-based, shear-strain calculation method as discussed by Cox et al. (2009). In Figure 11, examples are shown of derived time histories for pore-water pressure ratio and shear strain at two depths, 1.6 m and 2.1 m, in the 6-NS-1 test panel for the highest shaking level, ±107 kN. These results and other similar measurements were used to evaluate the r_u– logγ relationships at all PPTs in the test panels.

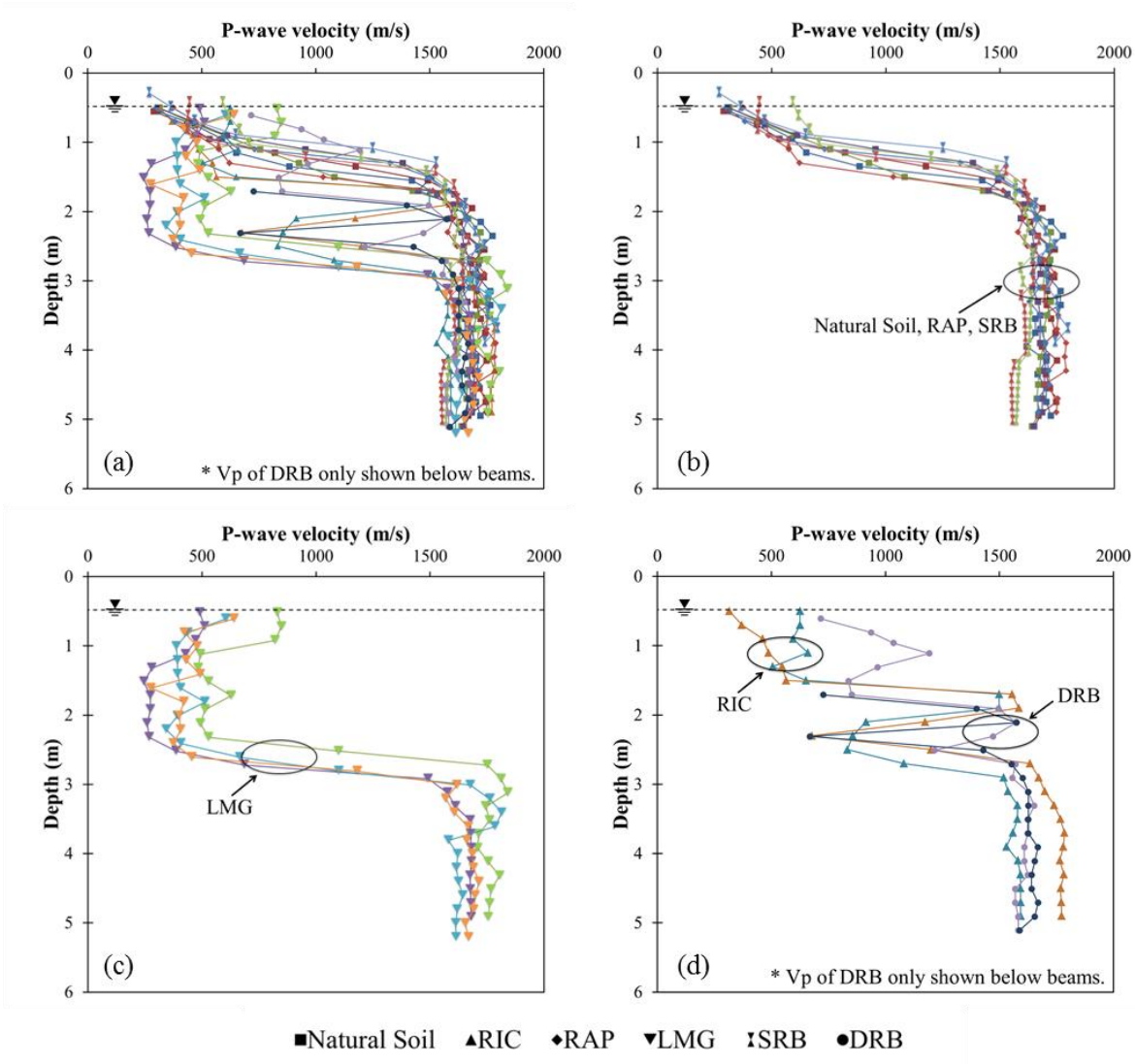

Figure 9: Profiles of compression (P) wave velocities at the seven test panels at Site 6: (a) two natural soil test panels, (b) between improvements at the RIC, RAP, SRB and LMG test panels, (c) across improvements at the SRB and DRB test panels and (d) across improvements at the RIC, RAP and LMG test panels.

It should be noted that cyclic stress ratios ($CSR = \tau/\sigma_v' = G\gamma/\sigma_v'$) are also shown in Figure 11. These values are peak values determined near the end of shaking. The values have been calculated using the general approach outlined in van Ballegooy et al. (2015a). The work with calculating the CSR values is under development and is not discussed further.

A. Pore water pressure ratio versus shear strain

In this work, the thrust of the T-Rex shaking tests was directed towards evaluating the r_u–logγ relationships at selected numbers of loading cycles (N) for each test panel. All data were reviewed and a generalized range in the r_u–logγ relationships was developed for the natural soils and soils at the improvement test panels that were >99.8% saturated and would have likely had liquefaction triggered in a "large" earthquake. At this time, the liquefaction-triggering has only been developed for N = 100 cycles. The range in r_u– logγ relationships is shown within the dashed zone in Figure 12. Data from Site 6 as well as Bexley Park (another near-by site tested by the UTexas team) that were used to develop the range are shown in the legend in Figure 12. Identifications of test panels, PPT sensors, PPT sensor depths and other information associated with the results presented in Figure 12 are summarized in Table 1.

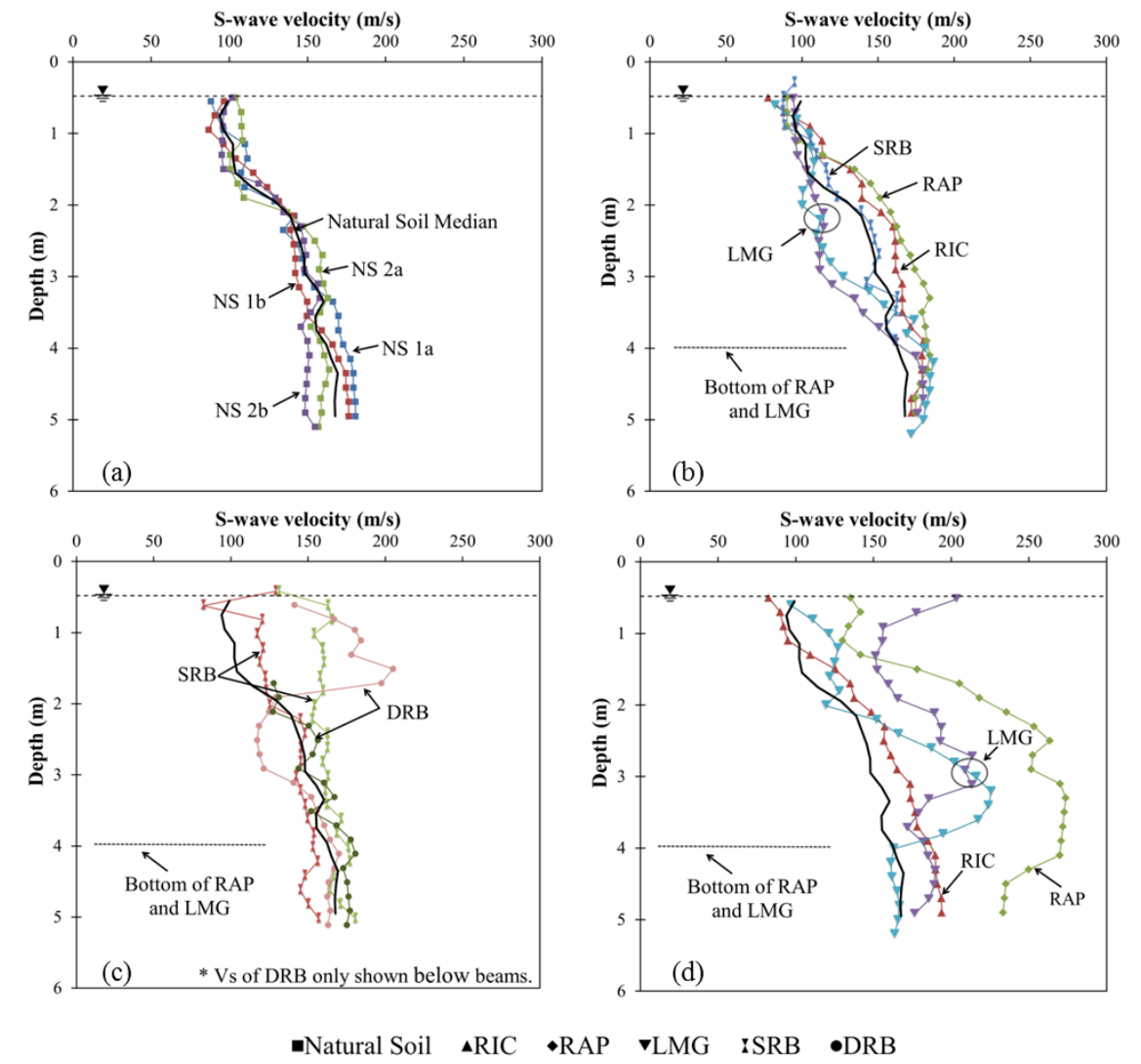

Figure 10: Profiles of shear (S) wave velocities at the seven test panels at Site 6: (a) two natural soil test panels, (b) between improvements at the RIC, RAP, SRB and LMG test panels, (c) across improvements at the SRB and DRB test panels and (d) across improvements at the RIC, RAP and LMG test panels.

All data exhibited a strong trend in the r_u–logγ relationships as follows. At low shear strains, strains below 0.01%, no excess pore-water pressure is generated ($r_u = 0$). As shear strain increases above some threshold, in the strain range of 0.01 to 0.04%, r_u begins to increase with increasing strain. The varying strain threshold is likely related to differences in material conditions and/or types. As r_u begins to exceed 20%, the values increase more rapidly and follow the general tread presented by Vucetic and Dobry (1986). Clearly, the trend in the r_u–logγ relationships indicated the potential for liquefaction triggering in a large earthquake.

B. Pore water pressure ratio versus shear strain

As presented by van Ballegooy et al. (2015a):

"The maximum γ for each loading stage was linearly adjusted slightly to [determine] a nominal level of applied shear stress at the ground surface so that the γ for each of the tested ground improvement panels could be directly compared. For example, the peak shear stress imparted by the T-Rex vibroseis unit at the ground surface during the second loading stage of the natural soil test panel at Site 6 [6-NS-1] was recorded as 5.3 kPa; therefore, the estimated peak γ for this loading stage were multiplied by

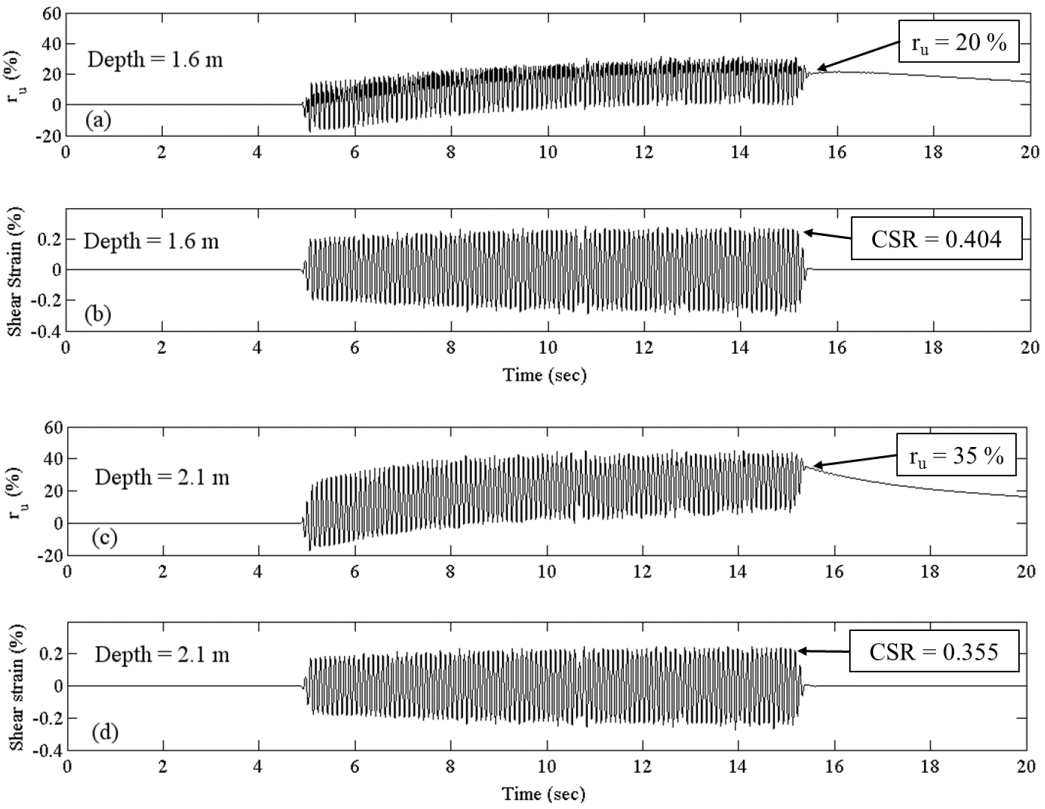

Figure 11: Variations of pore water pressure ratio, r_u, and shear, γ, strain with time determined from data recorded at the Natural Soil test panel (6 – NS-1) during T-Rex shaking at 10 Hz for 10 seconds; the final loading stage (± 107 kN) and PPT depths of 1.6 and 2.1 m. (Note: The values of Vp and Vs at each depth are presented in Table 1.)

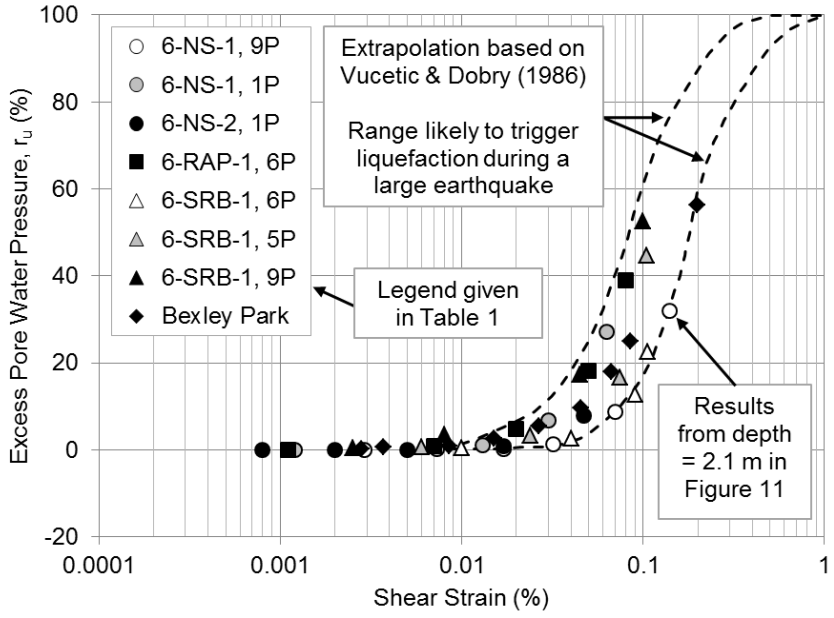

Figure 12: Compilation of T-Rex shaking results from five test panels that indicated soil liquefaction would likely be triggered in a large earthquake. (Note: The data for the 6-RAP-1 test panel is from a shallow depth of 1.15 m and likely results from the installation process loosening the shallow soil that had low confining stresses.)

Table 1: Identification of test panels, PPT sensors, PPT sensor depths and other information associated with the results presented in Figure 12.

Panel:	6-NS-1	6-NS-1	6-NS-2	6-RAP-1	6-SRB-1	6-SRB-1	6-SRB-1	Bexley Park
PPT Sensor:	9P	1P	1P	6P	6P	5P	9P	N/A
Depth (m):	2.1	2.85	2.9	1.15	1.3	1.55	2.05	2.25
σ_o' (kPa)	26.5	27.6	27.7	30.4	29.2	27.9	26.5	26.6
Vp (m/s):	1,700	1,730	1,617	1,180	1,460	1,490	1,650	1,500
Vs (m/s):	146	148	152	128	148	133	148	105

a ratio of 5 kPa : 5.3 kPa to linearly adjust the γ to match a nominal shear stress value for comparison across test panels. A nominal shear stress level is used because, while the input signal sent to T-Rex vibroseis unit is set at a consistent value for each test panel (e.g. 1.5, 5, 10, 15, 20 and 25 kPa), the true force output depends on the stiffness of the soil as well as various nonlinearities in the electrical and mechanical systems relating to the operation of the T-Rex vibroseis unit."

The relative stiffening effect of the RAP test panel relative to the two natural soil test panels at Site 6 is clearly shown in Figure 13, which was adapted from van Ballegooy et al. (2015a). In the first three loading stages, the stiffening effect reduced the shear strain in the soil between the RAP columns by more than 50 % on average. This effect is a topic of much interest in future studies.

V. CONCLUSION

Crosshole testing for pre-shaking characterization of the soil and T-Rex shaking to evaluate pore-pressure generation were successfully completed at seven test panels at Site 6. The field work provided strong evidence regarding soil liquefaction susceptibility of the natural soil as well as soil with ground improvements. The average water table depth at the seven test panels was approximately 0.5 m. Measurements of Vp showed that the point at which 100% saturation was continuous (not perched) ranged from depths of about 0.8 to 2.3 m below the water table. Relative changes in the value of Vs between different ground conditions (natural soil, soil between "improved" zones and soil within improved zones) were used to identify zones of improvement, zones of disturbance, and zones of little to no change.

Shaking with T-Rex generated substantial pore-water pressures at depth. The results from the shaking tests presented in this paper deal mainly with soils with Sr = 100%. The natural soil test panels exhibited significant variability in the pore pressure ratio versus log shear strain (r_u–logγ) relationships, with several layers predicted to have liquefaction triggered in a large earthquake and other layers predicted not to trigger. As evaluated by these tests, the ground improvement methods that inhibited liquefaction triggering the most were RIC, RAP, and DRB; the ground improvement methods that exhibited poor performance of inhibiting liquefaction triggering were LMG and SRB.

One additional benefit of T-Rex shaking the full-scale ground improvements was that the relative stiffening effect of the ground improvements could be evaluated. This effect was shown for the RAP test panel where the shear strains between the RAP columns were generally reduced by a factor of 1.5 or more compared with the Natural Soil test panels in the three loading stages before excess pore-water pressure began to be generated. It is planned to study this positive effect of ground improvements more in the future.

The Vp profiling by crosshole testing revealed that the crust (thickness ~0.65 m) was unsaturated. For the unsaturated crust with Vp less than about 600 m/s, T-Rex shaking tests showed that liquefaction triggering is unlikely, even in a large earthquake. T-Rex shaking trials showed a wide range in r_u–logγ relationships in the top 3 m that is likely due to differences in soil type, density, fabric, and/or degree of saturation.

Finally, the capability shown in the pre-shaking crosshole measurements to evaluate shear stiffness between improvements and shear stiffness across improvements has led to the adoption of this seismic method in New Zealand as one type of field verification procedure where shallow ground improvements are being installed.

ACKNOWLEDGEMENTS

Financial support for this study was provided through the National Science Foundation under grants from the RAPID program (CMMI-0343524), NEES@UTexas (CMMI-0927178), and the Graduate Research Fellowship Program (DGE-1110007). Other significant financial support was received from the New Zealand Earthquake Commission (EQC). This support is gratefully acknowledged.

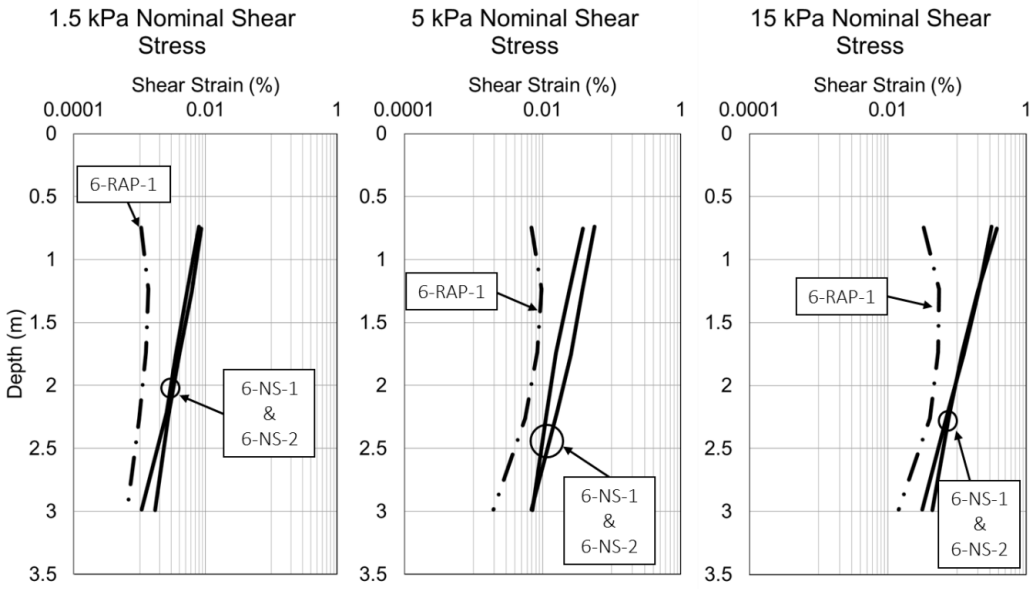

Figure 13: Relative stiffnesses of the RAP and natural soil test panels at Site 6 showing the stiffening effect of the RAP columns. Adapted from van Ballegooy et al. (2015a).

A special thanks is extended to the engineers and staff at Tonkin and Taylor Ltd. and to Prof. Misko Cubrinovski at the Univ. of Canterbury for their support throughout the project. Thanks also goes to graduate students and staff at the Univ. of Texas at Austin including Andrew Keene, Andrew Stolte, Mr. Cecil Hoffpauir, Mr. Andy Valentine, and Mr. Robert Kent. Finally, a significant portion of this paper was taken directly from an earlier publication (Stokoe et al., 2014) by the authors.

REFERENCES

[1] Andrus, D.R. and Stokoe, K. H., II. 2000. "Liquefaction Resistance of Soils from Shear-Wave Velocity," ASCE, *Journal of Geotechnical and Geoenvironmental Engineering*, Vol. 126, No. 11, pp 1015-1025.

[2] Bowen, H. J., Millar, P. J., Traylen, N. J. 2012. "Full Scale Testing of Ground Remediation Options for Residential Property Repair Following the Canterbury Earthquakes", in *New Zealand Society for Earthquake Engineering Annual Conference*. April 2012 Christchurch, New Zealand. 7 pp.

[3] Cox, B. R., Stokoe, K. H., II, Rathje, E. M. 2009. "An In-Situ Test Method for Evaluating the Coupled Pore Pressure Generation and Nonlinear Shear Modulus Behavior of Liquefiable Soils," *ASTM Geotechnical Testing Journal*. V. 32, No. 1, 11-21 pp.

[4] Cubrinovski, M., Henderson, D., Bradley, B. A. 2012. "Liquefaction Impacts in Residential Areas in the 2010-2011 Christchurch Earthquakes". *One Year after 2011 Great East Japan Earthquake: International Symp on Engrg. Lessons Learned from the Giant Earthquake*, March, 2012. Japan. 14 pp.

[5] Kayen R., Moss R., Thompson E., Seed R., Cetin K., Der Kiureghian A., Tanaka Y., Tokimatsu, K. (2013). Shearwave velocity–based probabilistic and deterministic assessment of seismic soil liquefaction potential, *J. Geotech. Geoenviron. Eng.*, 139(3): 407–419.

[6] Stokoe, K.H, II, Roberts, J., Hwang, S., Cox, B., Menq, F., & van Ballegooy, S. (2014). Effectiveness of inhibiting liquefaction triggering by shallow ground improvement methods: Initial field shaking trials with T-Rex at one site in Christchurch, New Zealand. In Orense, Towhata, & Chouw (Eds.), *Soil Liquefaction During Recent Large-Scale Earthquakes* (pp. 193-202). London: Taylor & Francis Group.

[7] Valle-Molina, C. (2006). Measurements of Vp and Vs in Dry, Unsaturated and Saturated Sand Specimens with Piezoelectric Transducers, Ph.D. Dissertation, The University of Texas, Austin, Texas.

[8] Valle-Molina, C., Stokoe, K.H., II (2012). Seismic Measurements in Sand Specimens With Varying Degrees of Saturation Using Piezoelectric Transducers. Canadian Geotechnical Journal, 49, pp 671-685.

[9] Van Ballegooy, S., Roberts, J.N., Stokoe, K.H. II, Cox, B.R., Wentz, F.J., Hwang, S., (2015a). "Large-Scale Testing of Shallow Ground Improvements

using Controlled Staged-Loading with T-Rex," 6th International Conference on Earthquake Geotechnical Engineering, Christchurch, New Zealand, November.

[10] Van Ballegooy, S., Wentz, F., Stokoe, K., Cox, B., Rollins, K., Ashford, S., & Olsen, M. (2015b). Christchurch Ground Improvement Trial Report. Report for the New Zealand Earthquake Commission. (In press).

[11] Vucetic, M. and Dobry, R. 1986. "Pore Pressure Build Up and Liquefaction at Level Sandy Sites During Earthquakes," Research Rpt., Depart. of Civil Engrg., Rensselaer Polytechnic Institute, Troy, New York.

[12] Wang, Y. (2015), Dynamic Properties of Fine Liquefiable Sand and Calcareous Sand from Resonant Column Testing, M.S. Thesis, The University of Texas at Austin, Austin, Texas.

[13] Wansbone, M., & van Ballegooy, S. (2015). Horizontal Soil Mixed Beam Ground Improvement as a Liquefaction Mitigation Method Beneath Existing Houses. 6th International Conference in Earthquake Geotechnical Engineering. Christchurch, New Zealand: ISSMGE.